Available online at www.sciencedirect.com
SCIENCE DIRECT®
Coordination Chemistry Reviews 246 (2003) 291–303
COORDINATION CHEMISTRY REVIEWS
www.elsevier.com/locate/ccr

Review

Photochemically degradable polymers containing metal–metal bonds along their backbones

David R. Tyler*

Department of Chemistry, University of Oregon, Eugene, OR 97403, USA

Received 15 April 2003; accepted 23 July 2003

Contents

Abstract

This review describes the synthesis and photochemistry of polymers that contain metal–metal bonds along their backbones. Such polymers are photodegradable because the metal–metal bonds are photolyzed by visible light. Understanding the factors that control the rate of polymer photodegradation is important for the technological applications of these materials, and this review focuses on two such factors, namely the radical cage effect and the applied stress on the polymer. With regard to the cage effect, data are reviewed showing that the k_d/k_c ratio (i.e. the ratio of the rate constant for diffusive separation out of the cage to that for radical–radical recombination in the cage) is proportional to $m^{1/2}/r^2$, where m is the mass of the radical fragment and r the radius. The effect of stress on a polymer undergoing degradation is to increase the initial separation of the radical particles following photolysis of a bond along the backbone. The increase in separation of the radicals decreases the likelihood of radical–radical recombination, leading to an increase in degradation efficiency. Quantitative knowledge of these and other factors that control polymer degradation will eventually allow synthesis of an ideal photodegradable polymer—one that has a tunable onset of degradation and that degrades quickly once degradation has started.

Keywords: Photodegradable polymer; Metal–metal bond; Cage effect; Stress effects; Radical–radical recombination

* Tel.: +1-503-346-4601; fax: +1-541-346-0487.
E-mail address: dtyler@darkwing.uoregon.edu (D.R. Tyler).

0010-8545/$ – see front matter © 2003 Elsevier B.V. All rights reserved.
doi:10.1016/S0010-8545(03)00127-9

1. Introduction

Photochemically reactive polymers [1–4] are of considerable interest because they are useful as photodegradable plastics [5], photoresists [6–10] biomedical materials, and as precursors to ceramic materials [6–8,11–14]. With regard to photodegradable plastics, it might seem strange to intentionally design a polymer material that falls apart when exposed to light, especially in view of the enormous efforts made by polymer chemists over the years to make their materials stable to light [1,2]. However, there are compelling economic and social reasons for using degradable plastics in certain applications and, therefore, considerable research is now devoted to devising new photodegradable polymers with improved performance [5]. The biggest use for photodegradable plastics is in agriculture, specifically in the burgeoning subdiscipline called plasticulture. In plasticulture, the ground is covered with plastic sheeting (typically a polyolefin), which acts as a mulch to prevent the growth of weeds (thus requiring the use of fewer herbicides), to decrease water demand, and to extend the growing season. By making these agricultural films out of degradable plastics, considerable labor and money can be saved in the plastics recovery phase of the technique. In the environmental area, photodegradable plastics are finding increased use as packaging materials in items that have a high probability of becoming litter. The idea is that if such materials should end up as litter they will degrade rather quickly and not be an eyesore.

There are two basic methods for making polymer materials photochemically degradable [1,2]. One method is to chemically incorporate a chromophore into the polymer chains. Although numerous chromophores have been evaluated, the most commercially successful chromophore is the carbonyl group [1,2,15]. Absorption of ultraviolet radiation leads to degradation by the Norrish Type I and II processes or by an atom abstraction process (Scheme 1), all of which are typical photoreactions of the carbonyl chromophore.

Initiation

Initiator ⟶ $R_i\bullet$

$R_i\bullet + O_2 \longrightarrow R_iOO\bullet$

$R_iOO\bullet + R{-}H \longrightarrow R_iOOH + R\bullet$

Propagation

$R\bullet + O_2 \longrightarrow ROO\bullet$

$ROO\bullet + R{-}H \longrightarrow R_iOOH + R\bullet$

Termination

various radical-radical coupling or disproportionation reactions

Scheme 2. The autooxidation mechanism for hydrocarbon materials.

Note that once radicals are introduced into the system, chain degradation can occur by the autooxidation mechanism (Scheme 2).

The second general method for making polymer materials photochemically degradable is to mix a radical initiator into the polymer. Once carbon-based radicals have formed, the chains degrade by the autooxidation cycle (Scheme 2). Numerous radical initiators have been investigated, and a partial list includes metal oxides (e.g. TiO_2, ZnO, CuO), metal chlorides (e.g. LiCl, $FeCl_3$), $M(acac)_n$ complexes, $M(stearate)_n$ complexes, benzophenone, quinones, and peroxides [1,2].

Both the carbonyl-containing and the radical initiator-containing types of degradable polymers require ultraviolet light for degradation. In order to expand the repertoire of photodegradable polymers to include those that degrade with visible light, we have been developing a new class of polymers that contain metal–metal bonded organometallic dimers interspersed along the polymer backbone [16–19]. These polymers are photodegradable because the metal–metal bonds can be cleaved with visible light and the resulting metal radicals captured with oxygen or other traps

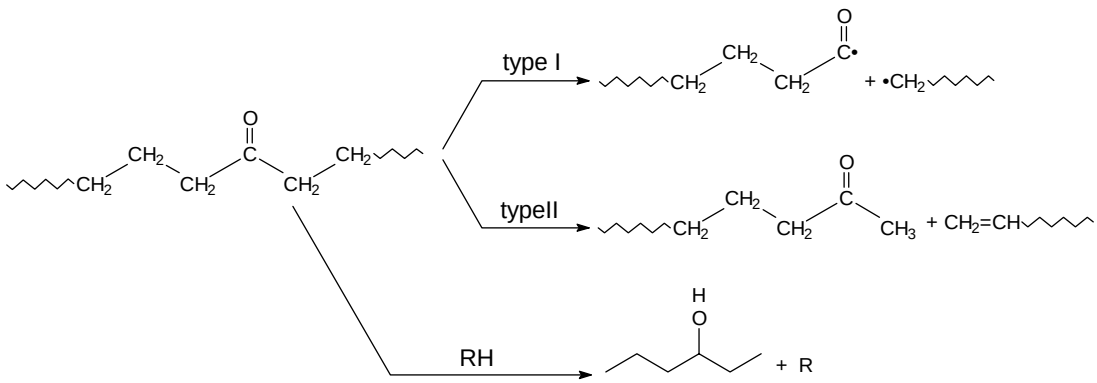

Scheme 1. Photochemical degradation pathways for polymers containing carbonyl groups.

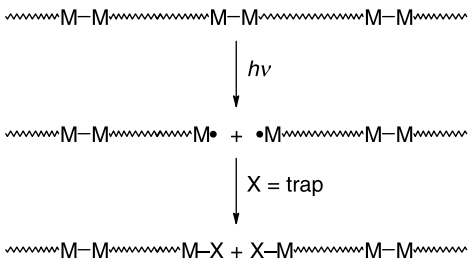

Scheme 3. Photochemical degradation of a polymer with metal–metal bonds along its backbone.

(Eq. (1) and Scheme 3) [20,21].

$$L_nM\text{–}ML_n \xrightarrow{h\nu} L_nM^{\bullet} + {}^{\bullet}ML_n$$

$${}^{\bullet}ML_n = CpMo(CO)_3 \quad (Cp = \eta^5\text{-}C_5H_5), \quad CpW(CO)_3, \quad Mn(CO)_5, \quad Re(CO)_5, \quad CpFe(CO)_2 \qquad (1)$$

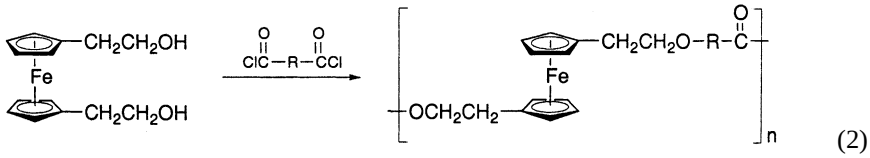

(2)

This review summarizes the work in our lab on photochemically degradable polymers that contain metal–metal bond chromophores. Our research is not necessarily intended to arrive at new commercial photodegradable polymers but to explore the photochemical mechanisms of decomposition, so that we and other workers will know what features and properties need to be incorporated into polymers to make them suitable as photodegradable materials. In this regard, it is noted that the ideal photodegradable polymer will degrade completely and quickly once degradation starts (Fig. 1). This characteristic makes practical sense, but it is also important for structural reasons because most polymer mechanical properties are related to molecular weight [22]. Small amounts of degradation can drastically decrease the molecular weight (and thus mechanical properties) of a plastic, yet to all appearances the plastic piece is visually unchanged. In essence, the plastic is still present but it is not structurally sound—and hence useless and perhaps dangerous. Under such circumstances, it may as well be completely degraded. A second ideal property is that the onset of degradation should be tunable. Again, this property makes practical sense, but it is difficult to achieve in practice because light intensities vary, as do temperatures and a host of other mechanistic variables.

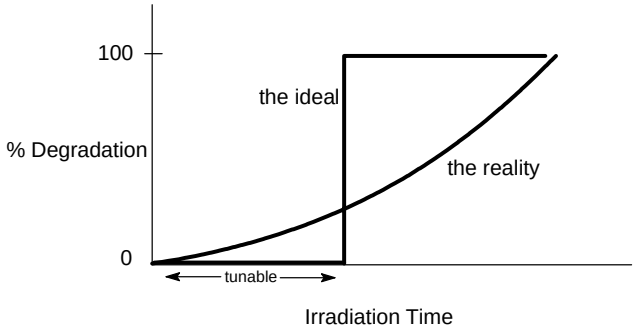

Fig. 1. A graph showing the properties of an ideal photochemically degradable polymer, namely tunable onset of degradable and rapid degradation.

2. Synthesis and characterization

Our general synthetic route for incorporating metal–metal bonds into polymer backbones is based on the step polymerization techniques for incorporating ferrocene into polymer backbones [23–29]. Step polymers of ferrocene can be made by substituting the Cp rings with appropriate functional groups, followed by reaction with appropriate difunctional organic monomers (e.g. Eq. (2)) [30–32].

The analogous strategy for synthesizing metal–metal bond-containing polymers also uses difunctional, cyclopentadienyl-substituted metal dimers. A sample polymerization reaction is shown in Eq. (3), which illustrates the reaction of a metal–metal bonded "diol" with hexamethylene diisocyanate (HMDI) to form a polyurethane (16).

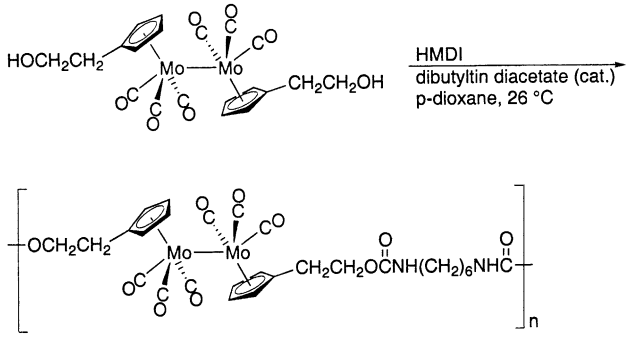

(3)

This step polymerization strategy is quite general, and a number of metal–metal bond-containing polymers have been made from monomers containing functionalized Cp ligands [23–29,33].

2.1. Synthesis of the difunctional dimers

The synthesis of metal–metal bonded dimers with functional groups substituted on the Cp rings is a synthetic challenge. The reason lies in the relative weakness of the metal–metal bonds ($D_{W–W} \approx 56\,kcal\,mol^{-1}$; $D_{Mo–Mo} \approx 32\,kcal\,mol^{-1}$ [34–36]). As they are relatively

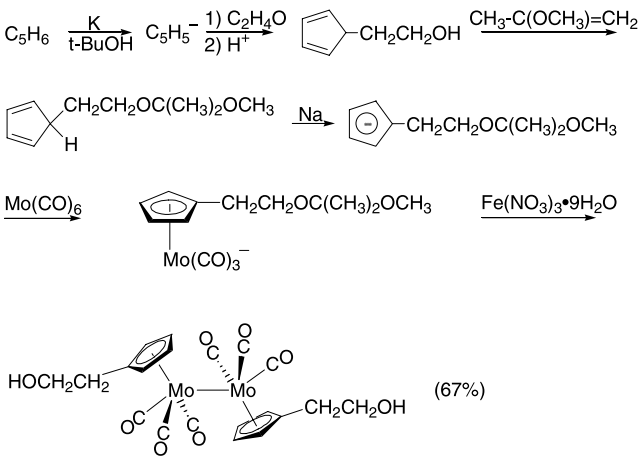

Scheme 4. Synthesis of an organometallic diol used in the polymer syntheses.

weak, the metal–metal bonds will not stand up to the harsh conditions typically required for the substitution of metal-coordinated Cp rings. For this reason, it is necessary to synthesize first the substituted Cp molecules and then coordinate these rings to the metals. High yield synthetic routes to alcohol- and amine-substituted Cp rings are summarized in Schemes 4 and 5 [16–18]. (The vinyl-substituted $Cp_2Fe_2(CO)_4$ dimer is an exception to this general synthetic strategy. The synthesis of $(Cp–CH{=}CH_2)_2Fe_2(CO)_4$ is discussed in the section following.) The routes to the difunctional dimer molecules are also shown in Schemes 4 and 5. (The analogous synthesis of a diacid functionalized W–W dimer is found in [37].) Note that the general route shown for the Mo-containing dimers (involving Fe^{3+} oxidation of the anionic species) was developed by Birdwhistell et al. [38]. The difunctional metal complex dimers were characterized by the usual spectroscopic methods, and it is worthy noting that the electronic absorption and infrared spectra in the ν(C=O) region are virtually identical to those of the unsubstituted dimers. The $(CpCH_2CH_2OH)_2Mo_2(CO)_6$ dimer was further structurally characterized by X-ray crystallography [39].

The synthesis of $(Cp–CH{=}CH_2)_2Fe_2(CO)_4$ is outlined in Scheme 6. The method involves the synthesis of the iodocyclopentadiene iron complex as outlined by Herrmann and Huber [40]. The vinyl group is then attached to the Cp by a palladium-catalyzed cross-coupling reaction [41], and finally the dimer is made by treatment with sodium naphthalide.

2.2. Synthesis of the polymers

Just as the comparatively weak metal–metal bonds pose problems for the synthesis of the difunctional dimers, they cause similar problems in the synthesis of the polymers. The relative weakness of the metal–metal bonds makes them more reactive than the bonds found in standard organic polymers; thus, under many standard polymerization reaction conditions, metal–metal bond cleavage would result. For example, metal–metal bonds react with acyl halides to form metal halide complexes. Therefore, the synthesis of polyamides using metal–metal bonded “diamines” and diacyl chlorides would simply lead to metal–metal bond cleavage rather than polymerization. Likewise, metal–metal bonded complexes are incompatible with many Lewis bases because the Lewis bases cleave the metal–metal bonds in disproportionation reactions [42]. This type of reactivity thus rules out many standard condensation polymerization reactions in which bases are used to neutralize any acids produced. Similar reasons prevent the use of acylchlorides in the synthesis of polyamides. All of the polymerization strategies are thus carefully designed to avoid cleaving the metal–metal bond during the polymerization process.

A sample polymerization reaction, showing the synthesis of a polyurethane, was shown above in Eq. (3). Using similar synthetic strategies, various polyurethanes, polyureas (e.g. Eq. (4)), polyvinyls (e.g. Eq. (5)), and polyamides (e.g. Eq. (6)) were synthesized [16–19]. Note that the step polymers in the various equations have a metal–metal bond in every repeat unit. Experiments showed that it was not necessary to have a metal–metal bond in every repeat unit in order to photochemically degrade the polymers [18]. Copolymers are straightforwardly synthesized by adding appropriate difunctional organic molecules into the reaction mixture.

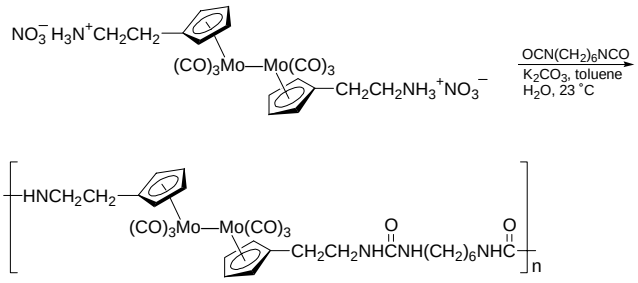

(4)

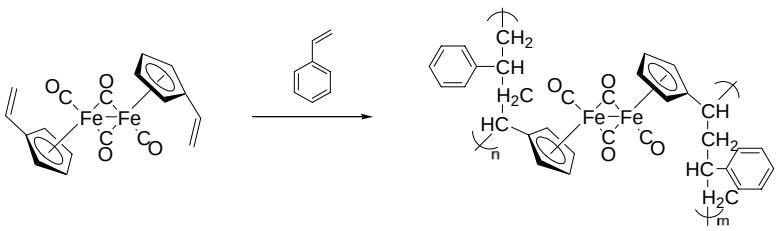

(5)

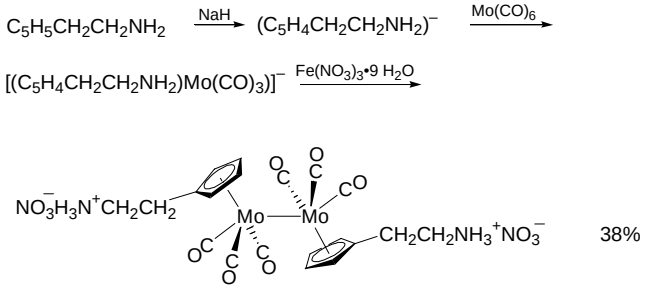

Scheme 5. Synthesis of an organometallic diamine used in the polymer syntheses.

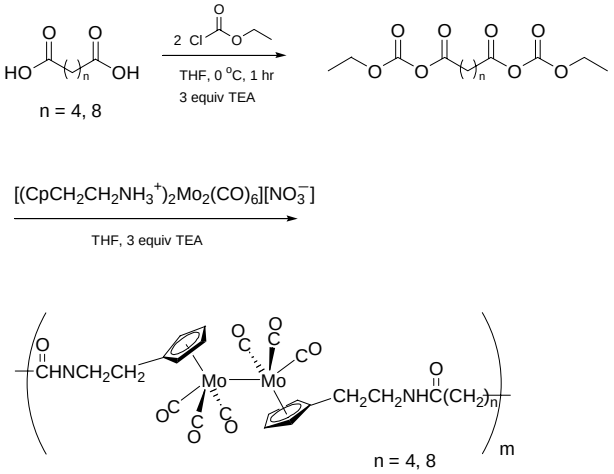

(6)

Yet another polymer synthesis strategy is to react the difunctional dimer molecules with prepolymers. Eq. (7) shows an example of this technique [18]. (In this instance, the prepolymer is one of the Hypol polymers sold by W.R. Grace. Analysis of the sample showed it to contain, on average, three tolyl isocyanate end groups; M_n was about 2000.)

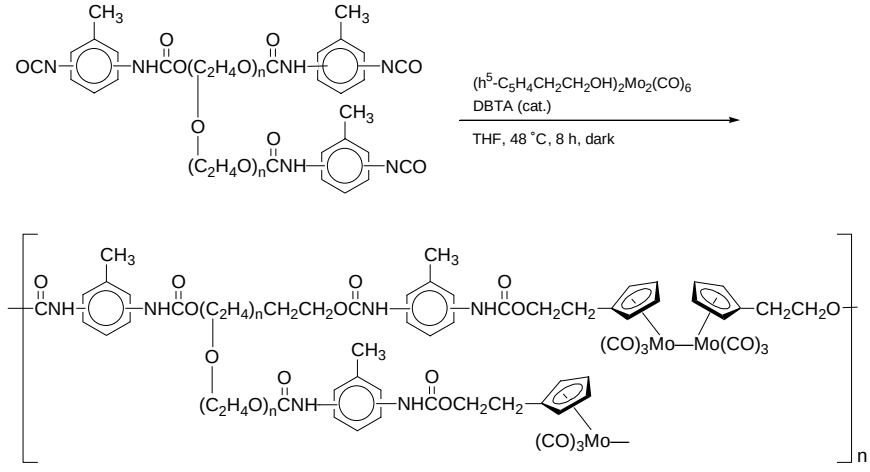

(7)

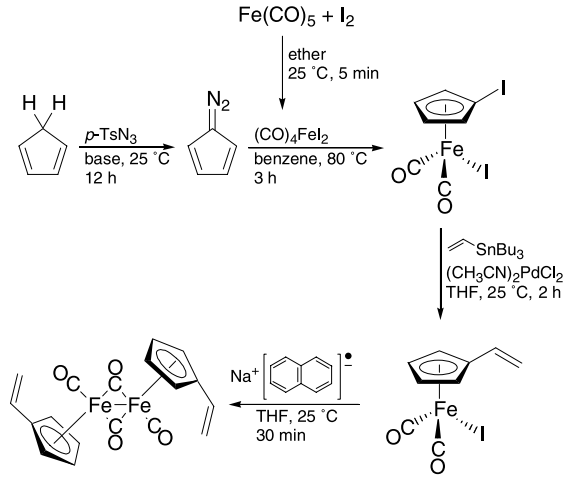

Scheme 6. Synthesis of an organometallic divinyl molecule used in the polymer syntheses.

2.3. Characterization of the polymers

The polymers were spectroscopically characterized by comparison of their infrared, electronic, and NMR spectra to model complexes [16–19]. For example, the product shown in Eq. (8), a model complex for the polymer in Eq. (3), was synthesized by reaction of $(CpCH_2CH_2OH)_2Mo_2(CO)_6$ with a mono-isocyanate (Eq. (8)).

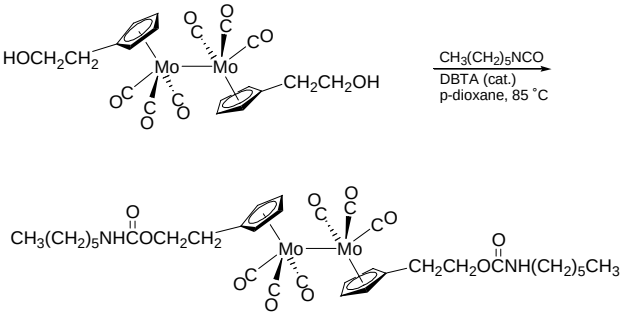

(8)

Typical M_n values, as measured by VPO or GPC, are between 5000 and 20,000 ($n = 7$–25). Thus, in many cases, the polymers are best described as oligomers. However, it is important to note that no effort was made to maximize the molecular weights.

3. Photochemical reactions in solution

Irradiation of metal–metal bonded complexes into their lowest energy absorption band (≈500 nm) generally leads to one of the three fundamental types of reactivity [16,20,21]. (1) The metal radicals produced by photolysis react with radical traps to form monomeric complexes (e.g. Eq. (9)). (2) The complexes react photochemically with ligands to form ionic disproportionation products (e.g., Eq. (10)). (3) The complexes react with oxygen to form metal oxides (Eq. (11)). (The latter reaction is likely a radical trapping reaction but may involve excited state electron transfer.) Note that higher energy excitation leads to M–CO bond dissociation. This type of reactivity is discussed below.

$$Cp_2Mo_2(CO)_6 + 2CCl_4 \xrightarrow{h\nu} 2CpMo(CO)_3Cl + 2[^{\bullet}CCl_3] \quad (9)$$

$$Cp_2Mo_2(CO)_6 + 2PR_3 \xrightarrow{h\nu} CpMo(CO)_3{}^- + CpMo(CO)_2(PR_3)_2{}^+ + CO \quad (10)$$

$$Cp_2Mo_2(CO)_6 \xrightarrow[O_2]{h\nu} \text{Mo oxides} \quad (11)$$

The qualitative photochemistry of the polymers in solution is analogous to the reactions of the discrete metal–metal bonded dimers in solution [16–19]. As in the photochemical reactions of the discrete dimers, the photochemical reactions of the polymers can be conveniently monitored by electronic absorption spectroscopy. The quantum yields for the reactions are in the range from ∼0.1 to 0.6, depending on the specific polymer and the M–M bond [17]. Sample reactions of the polymers showing the three types of reactivity are shown in Eqs. (12)–(14).

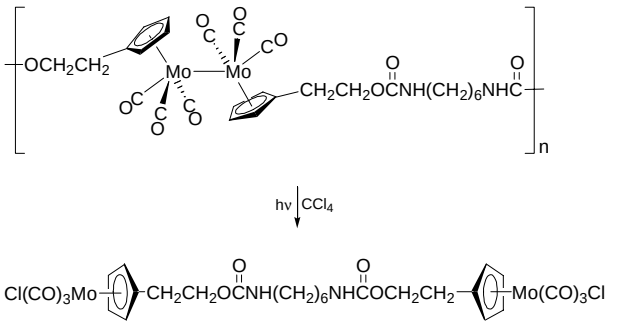

(12)

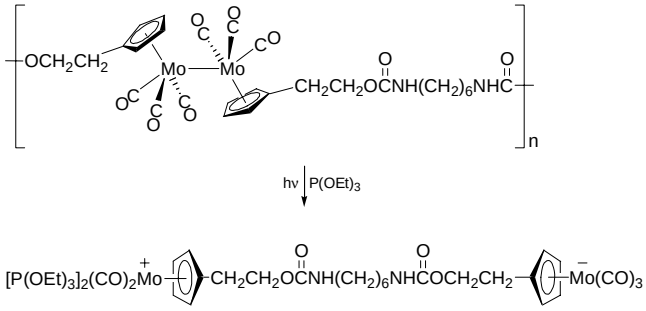

(13)

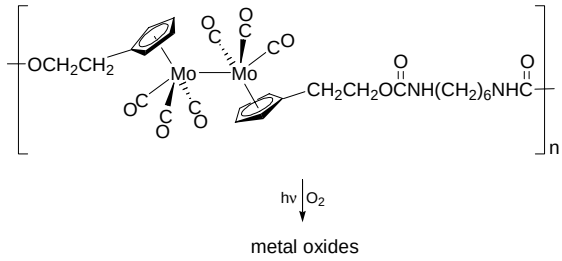

(14)

As mentioned, a fourth type of dimer reactivity is dissociation of a CO ligand from the dimer. Generally, this type of reactivity increases in efficiency relative to M–M photolysis as the radiation energy increases [20]. In solution, this type of reactivity generally leads to substitution. However, in the case of the $Cp_2Mo_2(CO)_6$ molecule, the reaction in Eq. (15) occurs [17]. (Among the dimers, this reaction to form a triply bonded product is unique to the Mo and W species.)

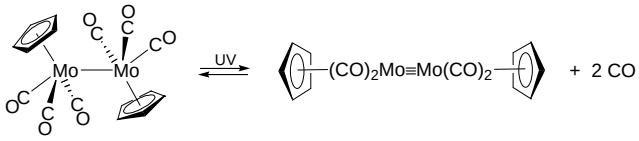

(15)

An analogous photoreaction occurs with polymers containing the Mo–Mo unit (Eq. (16)).

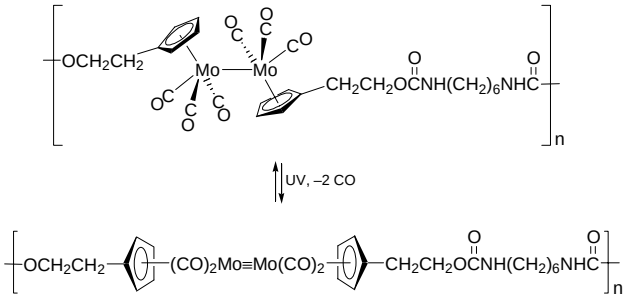

(16)

In both reactions 15 and 16, addition of CO to the product solution causes the system to back-react to reform the starting materials. Once again, the main point to be made is that

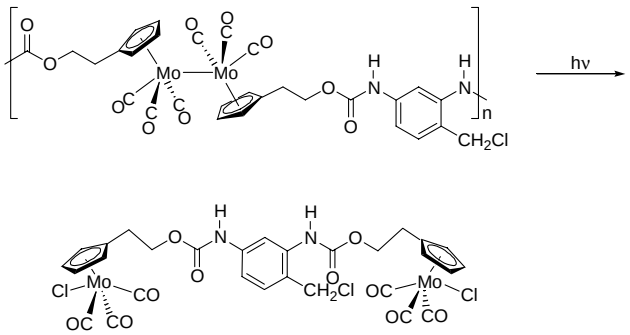

Scheme 7. Photochemical reaction of polymer **III** in the absence of an external trapping reagent.

the solution photochemistry of the polymers is analogous to the solution photochemistry of the discrete metal–metal bonded dimers. Photochemical reactivity in the absence of exogenous radical traps is possible in the case of polymers that have carbon–halogen bonds along their backbones. For example, irradiation of polymers **I–III** in solution in the absence of CCl_4 or O_2 led to net metal–metal bond cleavage [43]. Spectroscopic monitoring of the reaction showed that metal–metal bond cleavage is accompanied by an increase in the concentration of $CpMo(CO)_3Cl$ units. Photochemical reactions analogous to that in Scheme 7 were proposed.

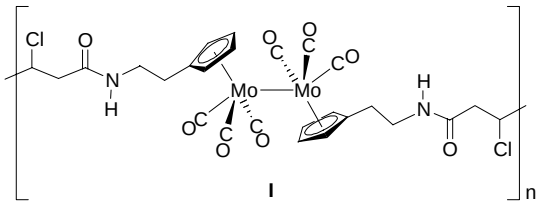

I

Further details of the polymer photochemistry are discussed in Section 5.

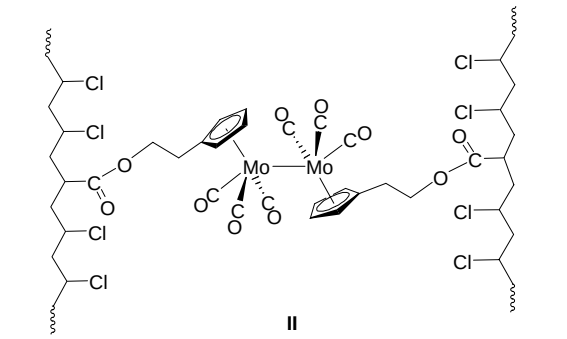

II

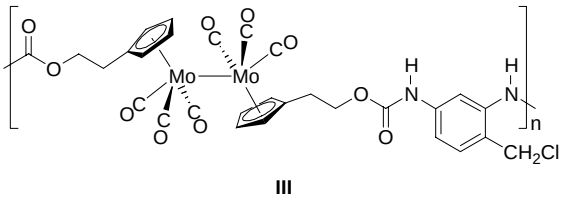

III

4. Photochemistry in the solid state

Thin films of the polymers (≈0.05 mm in thickness) reacted when they were exposed to *visible* light, whether from the overhead fluorescent lights in the laboratory, from sunlight, or from the filtered output of a high pressure Hg arc lamp [16–19]. All of the films were irradiated both in the presence and absence of oxygen. For each film and its dark reaction control, the absorbance of the $d\pi \rightarrow \sigma^*$ transition near 500 nm was monitored periodically over a period of several months. Fig. 2 is a plot of absorbance at 508 nm versus time for the polymer in Eq. (3) under the various experimental conditions. As indicated in figure, the polymer film that was exposed to sunlight in air completely decomposed in 2 months. (The $\sigma_{M-M} \rightarrow \sigma^*_{M-M}$ electronic absorption band at 390 nm disappeared during this time, confirming that the Mo–Mo bond was not intact.) Thin films stored in the dark in air or irradiated under nitrogen showed only a slight loss

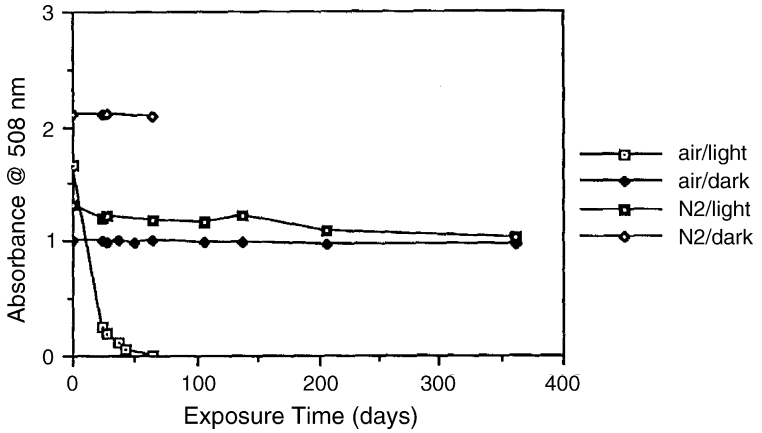

Fig. 2. A plot of the absorbance at 508 nm vs. time for four thin films of the polymer shown in Eq. (3). Only the sample exposed to both light and air degraded. The absorbance at 508 nm is characteristic of the metal–metal bond.

of absorbance at 508 nm over a 1-year period (Fig. 2). From this data, it was concluded that the decomposition of the polymers requires both light and air (oxygen). (The small amount of reaction for those slides stored in the glovebox in the light is probably due to reactions with solvent vapors.) Infrared spectra of the decomposition products showed the absence of products with CO ligands, as indicated by the absence of any stretches in the region 1600–2200 cm^{-1}. As mentioned previously, oxide complexes form in the solution phase reactions of $Cp_2Mo_2(CO)_6$ with O_2, and it was proposed that the metal-containing decomposition product of the polymer is a metal oxide.

These data suggest that oxygen is necessary for the solid-state photochemical reaction to occur. It was proposed that oxygen traps the metal radicals produced in the photolysis of the metal–metal bonds, thereby preventing radical recombination (Eq. (17)). If oxygen diffusion is rate-limiting then the relative rates of oligomer photochemical decomposition in the solid-state would reflect the oxygen diffusion rate.

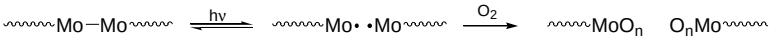

(17)

As described in the previous section, polymers **I–III** were designed to degrade in the absence of exogenous radical traps by building-in carbon–chlorine bonds along their backbones. As indicated, all of these polymers did degrade in the absence of oxygen when dissolved in solution, but only polymer **II** degraded in the solid state when irradiated in the absence of oxygen [43]. Apparently, only polymer **II** has a sufficiently high concentration of carbon–chlorine bonds to overcome the slow rate of diffusion in the solid state.

5. Factors controlling the rate of polymer photochemical degradation in solution

In order to synthesize a polymer material that has the ideal degradation properties shown in Fig. 1, it is first necessary to understand the factors control the rate of degradation. Mechanistic studies in the solid state are often difficult because the results can be difficult to interpret due to the plethora of variables. For that reason, the mechanistic photochemistry of the metal–metal bonded polymers was initially studied in the solution phase with the expectation that some of the factors that control the degradation rates in solution will also be important in the solid state.

Table 1
Quantum yields ($\lambda = 540$ nm) for the reactions of the indicated molecules with CCl_4 in hexane at 23 °C

Complex	Φ_{obsd}
$(CpR)_2Mo_2(CO)_6$	
R = $-CH_2CH_2OH$	0.66
R = $-CH_2CH_2OC(O)NH(CH_2)_6CH_3$	0.59
R = $-CH_2CH_2OC(O)NH(CH_2)_3-$	0.44
$(CpR)_2Fe_2(CO)_4$	
R = $-CH_2CH_2OH$	0.22
R = $-CH_2CH_2OC(O)NH(CH_2)_3-$	0.14

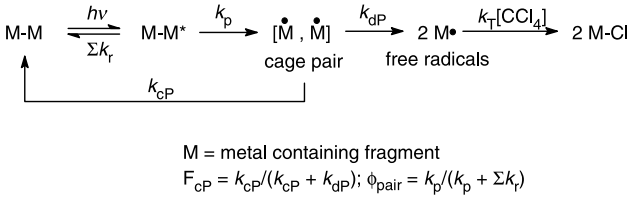

Scheme 8. Reaction scheme for metal–metal bond photolysis.

5.1. The cage effect

The quantum yields for photolysis of several dimers, model complexes, and polymers in 2 M CCl_4/THF are listed in Table 1. Note that the quantum yields vary as a function of molecular weight and size [18]; in general, longer chain species degrade with lower efficiency. This result may be general. Although other data are limited, one other example comes from the work of Guillet, who showed that the quantum yields for the Norrish Type I degradations of various model aliphatic ketones decreased as a function of chain length.[1] Reasons for the dependence of the quantum yields on the chain length have been a matter of considerable interest and speculation [44]. It is generally hypothesized that the dependence is attributable either to changes in ϕ_{pair} (the quantum yield for the formation of the radical cage pair; Scheme 8) or to changes in the "cage recombination efficiency" as the chain length is varied [45–47]. (The concept of the "cage effect" was introduced by Franck and Rabinowitch [45] in 1934 to explain why the efficiency of I_2 photodissociation was smaller in solution than in the gas phase. It was proposed that the solvent temporarily encapsulates the reactive $I^{\bullet}$ atoms in a "solvent cage", causing them to remain as colliding neighbors before they either recombine or diffuse apart. The point is that the formation of free radicals is preceded by the formation of a caged radical pair. The "cage recombination efficiency" (denoted as F_c) is defined as the ratio of the rate constant for cage recombination to the sum of the rate constants for all competing cage processes. The F_c value for a photochemically formed cage pair does not necessarily equal F_c for the same cage pair formed by thermolysis or by diffusional collision of two free radicals [48,49]. In order to differentiate these cases, the photochemical cage efficiency is denoted F_{cP} and the associated rate constants as k_{cP} and k_{dP}. In the photolysis reaction in Scheme 8, $F_{cP} = k_{cP}/(k_{cP} + k_{dP})$.)

[1] See [2], p. 274.

5.2. The effect of particle mass and size on the cage effect

In order to gain greater insight into the role that ϕ_{pair} and F_{cP} play in controlling the degradation of polymers, the model complexes $(CpCH_2CH_2OSiR_3)_2Mo_2(CO)_6$ (R = Me, *i*-Pr, *n*-Pr, *n*-Hx) were synthesized and studied [50,51]. As with the molecules discussed above, the overall quantum yields for these molecules decreased as the chain lengths increased. Furthermore, the cage recombination efficiencies increased as the chain lengths increased. Thus, the decrease in the overall quantum yield with increasing chain length can be at least partially attributed to an increase in F_{cP}. More specifically, k_d/k_c was found to be linearly proportional to $m^{1/2}/r^2$ (where m is the mass of the radical and r its radius). This result represented the first experimental verification of Noyes's prediction [52–56] concerning the relationship of particle mass and size to the cage effect.

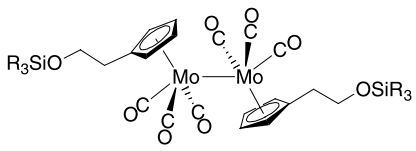

R = Me, *n*-Pr, *i*-Pr, *n*-Hx

In order to study the generality of the results obtained with the silylated molecules, additional model complexes of the type $(CH_3(CH_2)_nC(O)N(CH_3)CH_2CH_2Cp)_2Mo_2(CO)_6$ (n = 3, 8, 18) were synthesized, and F_{cP} was determined for each [57].

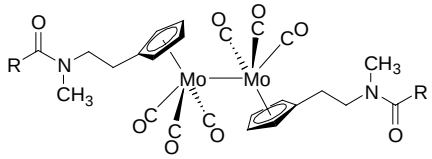

R = $(CH_2)_nCH_3$ with n = 3, 8 , and 18

As was the case for the silylated molecules, F_{cP} increased as the length of the chain increased, and again k_c/k_d was linearly proportional to $m^{1/2}/r^2$. Although this is just the second experimental verification of Noyes's prediction, the Noyes relationship is emerging as a rather general expression for predicting (or at least comparing) F_{cP} values.

The interesting feature about the reasonably good linear fit between k_d/k_c and $m^{1/2}/r^2$ for the radical cage pairs derived from the model complexes in the preceding paragraph is that Noyes derived his expression for spherical particles [52–56], yet the various radicals are decidedly not spherical. The explanation for the good fit lies in the reason for the dependence of F_{cP} on r^2. The parameter r^2 is proportional to the surface area of a particle, which in turn is proportional to the number of interactions a particle has with solvent molecules.

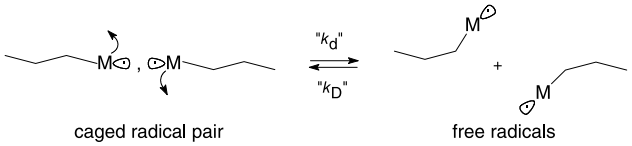

Fig. 3. Segmental motion leading to separation of two radicals in a radical cage pair.

The more interactions a particle has with the solvent, the greater the viscous drag and consequently the slower the rate of diffusion (and hence the inverse dependence of k_d/k_c on r^2). This analysis suggests that Noyes's expression can be modified by replacing r^2 with the particle's surface area, i.e. $k_d/k_c \propto m^{1/2}$/(radical surface area). In fact, plots of k_d/k_c versus $m^{1/2}$/(radical surface area) were linear [57]. As a further test, plots of k_d/k_c versus $m^{1/2}$/(radical surface area) were also linear for the $(CpCH_2CH_2OSiR_3)_2Mo_2(CO)_6$ molecules (R = Me, *i*-Pr, *n*-Pr, *n*-Hx). This result provided further support for the modified Noyes expression. The significance of being able to use a particle's surface area in the Noyes expression is that the expression becomes useful for non-spherical particles, i.e. it becomes possible to use the Noyes expression for virtually all radicals, not just spherical ones.

These results show that F_{cP} increases as the length of the chain on a radical center increases. In turn, this explains why the quantum yields for the photochemical degradation of polymers (and long-chain molecules, in general) decrease as the chains get longer. Undoubtedly, after a certain chain length is reached, no changes in F_{cP} will likely be observed due to the considerable inertia of the radicals. In such cases, the chain movements will be local, i.e. radical diffusion out of the cage or recombination in the cage will occur by segmental motion of the chain end and not by movement of the center of mass of the entire chain (Fig. 3). If such is the case then once a certain chain length is reached, additional chain length will not impact the segmental motion of the radical end [44].

6. Factors controlling the rate of polymer photochemical degradation in the solid state

6.1. The effect of stress

An interesting outcome of artificial weathering studies on polymers is the discovery that tensile- and shear-stress can accelerate the rate of photodegradation (for a review, see [58]). This phenomenon is general and has been observed with many polyolefins, including polystyrene [59,60], polypropylene [61–66], polyethylene [67–71], polyethylene–polypropylene copolymer [72], PMMA [73], and polyfluorocarbons [74], as well as with polycarbonates [65], nylons [75,76], acrylic–melamine coatings [77,78], and various elastomers and rubbers [79]. The occurrence of

stress-accelerated photodecomposition is a phenomenon of enormous practical importance because most polymers are subjected to light and some form of temporary or permanent stress during their lifetime. In order to control the rate of polymer photodegradation it is important to understand and control the enhanced degradation induced by the synergism of light and stress.

Why does stress cause changes in the photodegradation rates of polymers? Attempts to answer this question have generally been hampered by the mechanistic complexity of the degradation reactions [4]. Photochemical degradation pathways generally involve multiple steps, cross-linking, and side-reactions; these features make pinpointing the origin of stress-induced rate accelerations difficult. Another formidable complication is that oxygen diffusion is the rate-limiting step in many photooxidative degradations [70,80]. This adds to the intricacy of the analysis because oxygen diffusion rates are frequently time-dependent [80]. The metal–metal bond-containing polymers provide an exceptional method for studying this problem. As discussed above, when exposed to visible light, these polymers degrade by a straightforward mechanism involving metal–metal bond homolysis followed by capture of the metal radicals with a metal-radical trap (Scheme 3).

6.2. Mechanistic theories of stress effects on photodegradation

Mechanistic hypotheses to explain stress-accelerated photodegradation fall into two main categories. In one category, it is proposed that stress leads to an increase in the quantum yields for bond photolysis, i.e. it is proposed that $\phi_{\text{homolysis}}$ increases with stress (Eq. (18)). The other category attributes the increased degradation rates to a decrease in the efficiency of radical recombination following homolysis, i.e. $k_{\text{recombination}}$ is proposed to decrease as stress increases. The decreased efficiency of recombination is attributed to morphological changes in the polymer chain. The salient points of these theories are outlined in the following sections. Note that the following discussion is based on the assumption that radical trap diffusion is *not* the rate-limiting step.

(18)

6.2.1. The Plotnikov hypothesis

The Plotnikov hypothesis [81] attributes to the increase in degradation rates with applied stress to a decrease in the activation barrier for bond dissociation in the excited state. (See [81] for the appropriate pictures showing the differences in the potential energy surfaces for a stressed and unstressed bond.) Analysis of the potential energy surfaces for a stretched bond led Plotnikov to the following equation:

$$k_{\text{homolysis}} = k_0 \exp\left(-\frac{E_a}{T}\right),$$

$$\text{where } E_a = D\left[(1-\kappa)^{1/2} - \frac{\kappa}{2}\ln\frac{1+(1-\kappa)^{1/2}}{1-(1-\kappa)^{1/2}}\right], \quad (19)$$

and where $\kappa = f/F_m$, f is the stretching force on the bond, $F_m = \alpha D^*/2$, $\alpha = \omega[\mu/2D]^{1/2}$, μ the reduced mass, ω the bond vibration frequency, and D and D^* are the bond dissociation energies in the ground and excited states, respectively.

6.2.2. The decreased radical recombination hypothesis

Busfield and Monteiro [68], Benachour and Rogers [69], Nguyen and Rogers [82], Baimuratov et al. [83], and others in [84,85] proposed explanations for stress effects that are based on decreases in radical recombination efficiencies in stressed systems. In their models, the effect of stress is divided into four stages. Stage 1 represents the low stress domain. In this stage, there is only slight deformation of the original polymer structure and the rate of photodegradation is not greatly affected (Fig. 4). In Stage 2, higher stress causes significant morphological changes, including the straightening of the polymer chains in the amorphous regions. These straightened chains contain taut tie molecules. (Tie molecules are the interlamellar- or intercrystal-fibrils.) Macroscopic changes at these stress levels include the development of microcracks, crazes, and fissures. When bonds in the taut tie molecules are cleaved by light, the probability of radical recombination is decreased relative to non-stressed samples because entropic relaxation drives the radicals apart and prevents their efficient recombination. At slightly higher stresses (Stage 3), the chains are not only straightened but "stretched", and recoil aids in their separation (much like the mid-points of a stretched spring would fly apart if it were cut in the middle). According to this model, the diminished ability of the radicals to recombine is the primary reason that tensile stress will increase the rate of photodegradation.

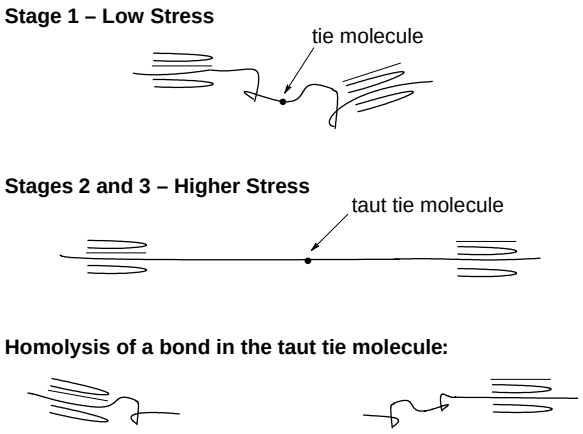

Fig. 4. The mechanistic origin of the decrease in radical–radical recombination in a stretched polymer.

Finally, in Stage 4 (not shown in Fig. 4), a strong stress is present which gives the polymer a fibrillar structure with a higher degree of orientation and crystallinity. Diffusion in a crystalline structure is retarded relative to the amorphous material, and the rate of degradation is expected to decrease slightly because of decreased trap mobility. Likewise, degradation rates will decrease in polymers with built-in radical traps because of decreased mobility in the crystalline phase. The polymers with metal–metal bonds along the backbone are beautifully set-up to probe this model of polymer degradation because simple homolytic scission of the chain occurs when they are irradiated.

6.2.3. The Zhurkov hypothesis

The last general hypothesis to explain the effect of stress on photodegradation rates is the photochemical analogue of the so-called Zhurkov equation. The effect of stress on the *thermal* degradation rates of polymers can be fitted to an *empirical* Arrhenius-like equation that is attributed to Zhurkov [58,86]:

$$\text{rate} = A \exp\left[-\left(\frac{\Delta G - B\sigma}{RT}\right)\right] \quad (20)$$

In this equation, ΔG is an "apparent" activation energy, σ the stress, and A and B are constants. It has been suggested that an equation similar to the Zhurkov equation might apply in photodegradations.

6.3. Photochemistry in the solid state

Polymer **II** can be used to eliminate the kinetically complicating effects of rate-limiting oxygen diffusion because it photochemically degrades in the absence of oxygen or other exogenous radical traps. As discussed above, of all the polymers containing Cl atoms attached to the polymer backbone, only this polymer degraded in the solid state when irradiated in the absence of exogenous radical trap [43]. In the case of those polymers that do not degrade in the solid state, it was concluded that, because of limited diffusion rates, the concentration of C–Cl bonds was too low to trap the radicals. In these cases, the radicals merely recombined, leading to no net degradation. However, thin films of **II** were photochemically reactive ($\lambda > 500$ nm) in the absence of oxygen. Infrared spectroscopic monitoring of the photochemical reaction showed the disappearance of the ν(C≡O) bands of the $Cp_2Mo_2(CO)_6$ moiety at 2009, 1952, and 1913 cm^{-1} and the appearance of bands attributed to the $CpMo(CO)_3Cl$ unit at 1967 and 2047 cm^{-1}. The application of tensile stress changed the photodegradation efficiency, and a plot of relative quantum yield versus stress is shown in Fig. 5. Note that tensile stress initially caused the quantum yield to increase, but after a certain point additional stress caused a decrease in the quantum yield.

These results are consistent with the "decreased radical recombination efficiency" hypothesis discussed above. All three hypotheses discussed above predict that stress will initially increase the efficiency of degradation, but only the "decreased radical recombination efficiency" hypothesis predicts that further increases in stress will eventually cause a decrease in photochemical efficiency. The conclusion, at least in this one system, is that the role of stress is to increase the separation of the photochemically generated radical pair, which decreases their probability of recombination. To our knowledge this is the first experimental confirmation of the behavior predicted by the "decreased radical recombination efficiency" hypothesis in which oxygen diffusion is not a complicating factor.

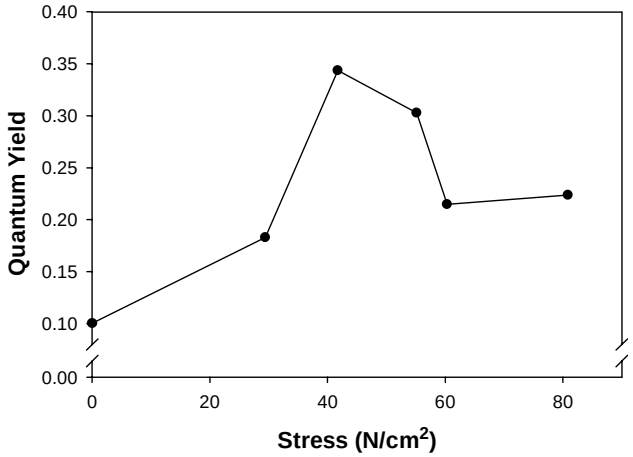

Fig. 5. Quantum yields for degradation of **II** vs. applied tensile stress. Quantum yield errors are estimated at ±5%.

X-ray scattering and infrared spectroscopy experimentally confirmed the increase in chain order in the stressed PVC polymer used in these experiments.

7. Summary

Step polymers containing metal–metal bonds along their backbones can be synthesized by reacting difunctional, cyclopentadienyl-substituted metal carbonyl dimers with appropriate difunctional organic molecules. A wide variety of polymers, including polyurethanes, polyureas, polyamides, and polyvinyls have been synthesized in a demonstration of the new synthetic method. Likewise, chain copolymers can be synthesized by reacting vinyl-substituted cyclopentadienyl metal carbonyl dimers with appropriate vinyl monomers. The polymers are photodegradable because the metal–metal bonds homolyze when irradiated with visible light. The photochemical reactions of the polymers in solution are identical to the photochemical reactions of the discrete metal–metal bonded dimers. Typical reactions include metal–metal bond disproportionation and chlorine atom abstraction from carbon tetrachloride. The polymers are also photochemically degradable in the solid state; thin films of the polymers degrade when irradiated with visible light in the presence of oxygen or if the polymer backbone

has a built-in radical trap. Although polymers containing metal–metal bonds are unlikely to find commercial applications, they are useful for studying the factors that control the rate of polymer photodegradation. The cage effect is one (of undoubtedly many) factor(s) that controls the degradation rate of polymers. In the solution phase, the ratio k_d/k_c is proportional to $m^{1/2}/r^2$, where m is the mass of the radical fragment and r the radius. In the solid state, stress on the polymer will increase the rate of degradation. Experiments show that the role of stress is to increase the separation of the radical fragments produced by photolysis. An increased separation leads to less radical–radical recombination, which increases the efficiency of degradation. Quantitative knowledge of these and other factors that control polymer degradation rates will eventually allow synthesis of an ideal photodegradable polymer—one that has a tunable onset of degradation and that degrades quickly once degradation has started.

Acknowledgements

Acknowledgment is made to the Donors of the Petroleum Research Fund, administered by the American Chemical Society, and to NSF (DMR-0096606 and CHE-0093869) for the support of the author's work reported herein.

References

[1] N. Grassie, G. Scott, Polymer Degradation and Stabilization, Cambridge University Press, New York, 1985.
[2] J. Guillet, Polymer Photophysics and Photochemistry, Cambridge University Press, Cambridge, 1985.
[3] J.F. Rabek, Mechanisms of Photophysical Processes and Photochemical Reactions in Polymers, Wiley, New York, 1987.
[4] G. Geuskens, in: C.H. Bamford, C.F.H. Tipper (Eds.), Comprehensive Chemical Kinetics, vol. 14, Elsevier, New York, 1975, pp. 333–424.
[5] J.E. Guillet, in: S.A. Barenberg, J.G. Brash, R. Narayan, A.E. Redpath (Eds.), Degradable Materials, CRC Press, Boston, 1990, pp. 55–97.
[6] R. West, J. Maxka, in: M. Zeldin, K.J. Wynne, H.R. Allcock (Eds.), Inorganic and Organometallic Polymers, ACS Symposium Series 360, American Chemical Society, Washington, DC, 1988, Chapter 2.
[7] R. West, L'actualite Chim. (1984) 64.
[8] R.J. West, J. Organomet. Chem. 300 (1986) 327.
[9] D.C. Hoger, R.D. Miller, C.G. Wilson, A.R. Neureuther, SPIE, Adv. Resist. Technol. 469 (1984) 108.
[10] M. Ishikawa. K. Nate, in: M. Zeldin, K.J. Wynne, H.R. Allcock (Eds.), Inorganic and Organometallic Polymers, ACS Symposium Series 360, American Chemical Society, Washington, DC, 1988, Chapter 16.
[11] S. Yajima, J. Hayashi, M. Omori, Chem. Lett. (1975) 931.
[12] S. Yajima, Ceram. Bull. 62 (1983) 893.
[13] R.M. Laine, Y.D. Blum, D. Tse, R. Glaser, in: M. Zeldin, K.J. Wynne, H.R. Allcock (Eds.), Inorganic and Organometallic Polymers, ACS Symposium Series 360, American Chemical Society, Washington, DC, 1988, Chapter 10.
[14] D. Gilead, in: S.A. Barenberg, J.G. Brash, R. Narayan, A.E. Redpath (Eds.), Degradable Materials, CRC Press, Boston, 1990, pp. 191–207.
[15] P.J. Hocking, J. Macromol. Sci., Rev. Macromol. Chem. Phys. C32 (1992) 35.
[16] S.C. Tenhaeff, D.R. Tyler, Organometallics 10 (1991) 473.
[17] S.C. Tenhaeff, D.R. Tyler, Organometallics 10 (1991) 1116.
[18] S.C. Tenhaeff, D.R. Tyler, Organometallics 11 (1992) 1466.
[19] G.F. Nieckarz, D.R. Tyler, Inorg. Chim. Acta 242 (1996) 303.
[20] T.J. Meyer, J.V. Caspar, Chem. Rev. 85 (1985) 187.
[21] G.L. Geoffroy, M.S. Wrighton, Organometallic Photochemistry, Academic Press, New York, 1979.
[22] G. Odian, Principles of Polymerization, third ed., Wiley–Interscience, New York, 1991.
[23] C.U. Pittman Jr., M.D. Rausch, Pure Appl. Chem. 58 (1986) 617.
[24] K. Gonsalves, L. Zhan-ru, M.D. Rausch, J. Am. Chem. Soc. 106 (1984) 3862.
[25] K.E. Gonsalves, R.W. Lenz, M.D. Rausch, Appl. Organomet. Chem. 1 (1987) 81.
[26] F.W. Knobloch, W.H. Rauscher, J. Polym. Sci. 54 (1961) 651.
[27] C.U. Pittman Jr., J. Polym. Sci. (Part A) 6 (1968) 1687.
[28] K.E. Gonsalves, M.D. Rausch, J. Polym. Sci., Part A: Polym. Chem. 26 (1988) 2769.
[29] W.J. Patterson, S.P. McManus, J. Polym. Sci., Part A: Polym. Chem. 12 (1974) 837.
[30] P. Nguyen, P. Gomez-Elipe, I. Manners, Chem. Rev. (Washington, DC) 99 (1999) 1515.
[31] I. Manners, Adv. Organomet. Chem. 37 (1995) 131.
[32] I. Manners, Coord. Chem. Rev. 137 (1994) 109.
[33] M. Moran, M.C. Pascual, I. Cuadrado, J. Losada, Organometallics 12 (1993) 811.
[34] J.R. Krause, D.R. Bininosti, Can. J. Chem. 53 (1975) 628.
[35] J.T. Landrum, C.D. Hoff, J. Organomet. Chem. 282 (1985) 215.
[36] S. Amer, G. Kramer, A.J. Poë, J. Organomet. Chem. 209 (1981) C28.
[37] A. Avey, S.C. Tenhaeff, T.J.R. Weakley, D.R. Tyler, Organometallics 10 (1991) 3607.
[38] R. Birdwhistell, P. Hackett, A.R. Manning, J. Organomet. Chem. 157 (1978) 239.
[39] S.C. Tenhaeff, D.R. Tyler, T.J.R. Weakley, Acta Crystallogr. C 47 (1991) 303.
[40] W.A. Herrmann, M. Huber, Chem. Ber. 111 (1978) 3124.
[41] E.C. Brehm, J.K. Stille, A.I. Meyers, Organometallics 111 (1992) 938.
[42] A.E. Stiegman, D.R. Tyler, Coord. Chem. Rev. 63 (1985) 217.
[43] M. Yoon, D.R. Tyler, unpublished work.
[44] J. Guillet, Adv. Photochem. 14 (1988) 91.
[45] J. Franck, E. Rabinowitch, Trans. Faraday Soc. 30 (1934) 120.
[46] E. Rabinowitch, W.C. Wood, Trans. Faraday Soc. 32 (1936) 1381.
[47] E. Rabinowitch, Trans. Faraday Soc. 33 (1937) 1225.
[48] T. Koenig, H. Fischer, in: J. Kochi (Ed.), Free Radicals, vol. 1, Wiley, New York, 1973, Chapter 4.
[49] T. Koenig, in: W.A. Pryor (Ed.), Organic Free Radicals, ACS Symposium Series 69, 1978, Chapter 9.
[50] J.L. Male, B.E. Lindfors, K.J. Covert, D.R. Tyler, Macromolecules 30 (1997) 6404.
[51] J.L. Male, B.E. Lindfors, K.J. Covert, D.R. Tyler, J. Am. Chem. Soc. 120 (1998) 13176.
[52] R.M. Noyes, J. Chem. Phys. 22 (1954) 1349.
[53] R.M. Noyes, Prog. React. Kinet. 1 (1961) 129.
[54] R.M. Noyes, J. Am. Chem. Soc. 77 (1955) 2042.
[55] R.M. Noyes, J. Am. Chem. Soc. 78 (1956) 5486.
[56] R.M. Noyes, Z. Elektrochem. 64 (1960) 153.
[57] E. Schutte, T.J.R. Weakley, D.R. Tyler, J. Am. Chem. Soc. 125 (2003) 10319.
[58] J.R. White, N.Y. Rapoport, Trends Polym. Sci. (Cambridge, UK) 2 (1994) 197.
[59] B. O'Donnell, J.R. White, J. Mater. Sci. 29 (1994) 3955.
[60] B. O'Donnell, J.R. White, Polym. Prepr. (Am. Chem. Soc., Div. Polym. Chem.) 34 (1993) 137.
[61] L. Tong, J.R. White, Polym. Degrad. Stab. 53 (1996) 381.
[62] R.B. Neto, M. De Paoli, Polym. Degrad. Stab. 40 (1993) 59.
[63] R.B. Neto, M. De Paoli, Polym. Degrad. Stab. 40 (1993) 53.

[64] G.E. Schoolenberg, P. Vink, Polymer 32 (1991) 432.
[65] C.T. Kelly, L. Tong, J.R. White, J. Mater. Sci. 32 (1997) 851.
[66] B. O'Donnell, J.R. White, Polym. Degrad. Stab. 44 (1994) 211.
[67] C.T. Kelly, J.R. White, Polym. Degrad. Stab. 56 (1997) 367.
[68] W.K. Busfield, M. Monteiro, J. Mater. Forum 14 (1990) 218.
[69] D. Benachour, C.E. Rogers, in: Proceedings of the ACS Symposium Series on Photodegradation and Photostabilization of Coatings, ACS Symposium Series 151, American Chemical Society, Washington, DC, 1981, p. 263.
[70] M. Igarashi, K.L. DeVries, Polymer 24 (1983) 1035.
[71] A. Huvet, J. Philippe, J. Verdu, Eur. Polym. J. 14 (1978) 709.
[72] W.K. Busfield, P. Taba, Polym. Degrad. Stab. 51 (1996) 185.
[73] F. Thominette, J. Verdu, Polym. Prepr. (Am. Chem. Soc., Div. Polym. Chem.) 35 (1994) 971.
[74] V.I. Tupikov, S.A. Khatipov, V.F. Stepanov, Phys. Chem. Mater. Treatment 31 (1997) 32.
[75] M. Igarashi, K.L. DeVries, Polymer 24 (1983) 769.
[76] H. Matsui, S.M. Arrivo, J.J. Balentini, J.N. Weber, Macromolecules 33 (2000) 5655.
[77] M.E. Nichols, J.L. Gerlock, C.A. Smith, Polym. Degrad. Stab. 56 (1997) 81.
[78] T.-L.H. Nguyen, C.E. Rogers, Sci. Eng. 56 (1987) 589.
[79] C.M. Maillo, J.R. White, Plast. Rubber Compos. 28 (1999) 277.
[80] J. Malik, A. Hrivik, D.Q. Tuan, in: R.L. Clough, N.C. Billingham, K.T. Gillen (Eds.), Polymer Durability, American Chemical Society, Washington, DC, 1996, pp. 455–471 (see p. 459 in particular).
[81] V.G. Plotnikov, Proc. Acad. Sci. USSR, Phys. Chem. Sect. 301 (1989) 618 (English Translation of V.G. Plotnikov, Dokl. Akad. Nauk. SSSR 301 (1988) 376).
[82] T.-L. Nguyen, C.E. Rogers, Sci. Eng. 53 (1985) 292.
[83] E. Baimuratov, D.S. Saidov, I.Y. Kalontarov, Polym. Degrad. Stab. 39 (1993) 35.
[84] Y.A. Shlyapikov, S.G. Kiryushkin, A.P. Marin, Antioxidative Stabilization of Polymers, Taylor and Francis, Bristol, PA, 1996.
[85] J.F. Rabek, Photostabilization of Polymers, Elsevier, New York, 1990.
[86] S.N. Zhurkov, V.A. Zakrevskyi, V.E. Korsukov, A.F. Kujsenko, J. Polym. Sci. Part A-2: Polym. Phys. Ed. 10 (1972) 1509.